Energy Conversion and Management 87 (2014) 990–999

Contents lists available at ScienceDirect

Energy Conversion and Management

journal homepage: www.elsevier.com/locate/enconman

Economic emission dispatching with variations of wind power and loads using multi-objective optimization by learning automata

H.L. Liao [a], Q.H. Wu [a,b,*], Y.Z. Li [a], L. Jiang [b]

[a] School of Electric Power Engineering, South China University of Technology, Guangzhou 510640, Guangdong, PR China
[b] Department of Electrical Engineering and Electronics, University of Liverpool, Liverpool L69 3GJ, UK

ARTICLE INFO

Article history:
Received 2 August 2013
Accepted 28 July 2014
Available online 27 August 2014

Keywords:
Multi-objective optimization
Economic emission dispatch
Voltage stability enhancement
Learning automata
Dimensional search
State memory

ABSTRACT

This paper is concerned with using multi-objective optimization by learning automata (MOLA) for economic emission dispatching in the environment where wind power and loads vary. With its capabilities of sequentially dimensional search and state memory, MOLA is able to find accurate solutions while satisfying two objectives: fuel cost coupled with environmental emission and voltage stability. Its searching quality and efficiency are measured using the hypervolume indicator for investigating the quality of Pareto front, and demonstrated by tracking the dispatch solutions under significant variations of wind power and load demand. The simulation studies are carried out on the modified midwestern American electric power system and the IEEE 118-bus test system, in which wind power penetration and load variations present. Evaluated on these two power systems, MOLA is fully compared with multi-objective evolutionary algorithm based on decomposition (MOEA/D) and non-dominated sorting genetic algorithm II (NSGA-II). The simulation results have shown the superiority of MOLA over NAGA-II and MOEA/D, as it is able to obtain more accurate and widely distributed Pareto fronts. In the dynamic environment where the operation condition of both wind speed and load demand varies, MOLA outperforms the other two algorithms, with respect to the tracking ability and accuracy of the solutions.

1. Introduction

Power system dispatch is, in essence, a multi-objective optimization problem. For instance, one of the dispatch problem, optimal power flow (OPF), aims to achieve optimal solutions (Pareto solutions) as for multiple objective functions, such as fuel cost reduction, emission reduction, power loss minimization and voltage stability enhancement [1–4]. Nowadays, with large amount of wind power embedded in power systems, dispatch problems confront new challenges, as wind power penetration brings instability and complexity to the power system dispatching [5,6], in particular in the environment where there are load variations. Among the multiple objectives, two are important to power system operation, which are considered in this paper. The first objective is to reduce fuel cost and pollutant emission, which is widely known as economical and environmental problems, *i.e.* economic emission dispatch problem [1,3,7]. The second objective is to enhance voltage stability, this is because the instability of voltage would lead to severe detriments to power system operation, and the index of voltage stability is usually optimized as for power system dispatch problems [2–4,8,9].

In the last decade, various multi-objective optimization algorithms have been comprehensively investigated, including multi-objective evolutionary algorithms [1–4,10–14]. However, to deal with power system dispatch problems, they suffer the drawback of computational burden. This drawback mainly results from their use of population-based search approach in which there is a high level of randomness. Besides, using a large population leads to a certain degree of overlapped search, and thus results in inefficiency during the search, especially in dynamic environment. For instance, varying wind power and load demand bring a great challenge in dispatching, evolutionary algorithms have a limited capability of tracking the varying operation condition because of their random searching mechanism [15].

Learning automata (LA) is an alternative way to evolutionary algorithms in dealing with optimization problems. It aims to achieve the desired goal and is based on modifying its strategy (i.e. changing its structure and parameters) by learning its experience obtained from processing current information about the environment [16]. As for its application, for instance, the continuous-action learning automata has been applied for stochastic optimization [17,18], the genetic learning automata was proposed to solve

* Corresponding author at: School of Electric Power Engineering, South China University of Technology, Guangzhou 510640, Guangdong, PR China.
E-mail address: wuqh@scut.edu.cn (Q.H. Wu).

http://dx.doi.org/10.1016/j.enconman.2014.07.071
0196-8904/

function optimization problems [19]. However, a few LA methods have been investigated to solve multi-objective optimization problems [20], especially as for power system dispatching. In [21], LA and genetic algorithms are combined to solve the multi-objective generation dispatch. In [17], a S-model LA method is used to determine the optimal operation of a power system, by considering its economy and stability. However [21,17], only considers a small system, as LA requires a huge amount of computation caused by the large number of states involved in the continuous search, if the dimensionality of the decision space increases.

To avoid the huge amount of computation [20], proposes a novel method for multi-objective optimization by learning automata (MOLA). The decision space is divided into multiple dimension, and each learning automata is used to take actions regarding to its corresponding dimension. Furthermore, each dimension is divided into a certain number of cells for further search. The effectiveness of MOLA has been proved comprehensively by testing a series of benchmark functions and a simple power system benchmark. However, it has not well demonstrated the potential of MOLA's application in power system [20], as for the dynamic environment of uncertain wind power and loads are not considered.

Therefore, this paper presents MOLA to solve the optimal multi-objective dispatch problem, considering economic emission dispatch and voltage stability enhancement in dynamic environments where wind power and loads vary. MOLA consists of multiple automata, where each automaton undertakes dimensional search on a selected dimension of the solution domain. With the ability of learning and memorization, MOLA has been found capable of tracking accurate solutions, in an efficient way, to the multi-objective dispatch problems with the variation of the operation conditions of power systems. With the approach of sequential search of all control variables, the power system has superior performance with respect to voltage stability during the process of optimization. In this paper, the investigation is carried out on the modified mid-western American electric power system and the IEEE 118-bus test power system, which are penetrated with varying wind power and load demand. The merits of MOLA have been demonstrated through comparison with non-dominated sorting genetic algorithm II (NSGA-II) [12] and multi-objective evolutionary algorithm based on decomposition (MOEA/D) [11,22]. In dynamic environment, MOLA is able to track the varying operation condition of both wind power penetration and load demand more quickly and accurately, in comparison with the other two algorithms. The hypervolume indicator is introduced to investigate the quality of Pareto front approach and search capability of MOLA.

2. Problems formulation

2.1. Wind power penetration

The power output of a wind turbine is determined by the wind speed at the location where it is installed. A relationship between the power generated and the wind speed has been proposed in the research of [23]. Then, the active power output of a wind turbine can be formulated as:

$$P_{wt}=\begin{cases}0 & 0\leqslant v<v_{ci}\\ a+bv^3 & v_{ci}\leqslant v<v_{ra}\\ P_{ra} & v_{ra}\leqslant v\leqslant v_{co}\\ 0 & v>v_{co}\end{cases} \tag{1}$$

$$a=\frac{P_{ra}v_{ci}^3}{v_{ci}^3-v_{ra}^3};\quad b=\frac{P_{ra}}{v_{ra}^3-v_{ci}^3} \tag{2}$$

where v denotes the wind speed, v_{ci} is the cut-in wind speed, v_{ra} is the rated wind speed, v_{co} is the cut-out wind speed, and P_{ra} is the rated power of wind turbine. It is assumed that only one type of variable-speed wind turbines is used in this paper. The rate power of wind turbine is set to be 2 MW, the rated wind speed is set to be 12.5 m/s, the cut-in and cut-out wind speed are set to be 4 m/s and 20 m/s, respectively.

When wind power is penetrated into a power system, the power flow calculation will be affected by the characteristic of the wind turbines. Generally, multiple wind turbine generators are embedded into a power grid in the form of the wind farm. Thus, the model of wind farm which aggregates multiple wind turbine generators (variable-speed wind turbine generators are concerned in the paper) is required. The simplest variable-speed aggregate model to construct is the one that represents the wind farm as a single equivalent wind turbine generator. Since the aggregation procedure is applied to groups of similar wind turbines in areas of the power system, the equivalent wind turbine to the entire wind farm is a scale up of a single wind turbine, whose wind power becomes the sum of the wind power generated by all the wind turbines in the wind farm [24,25]. This aggregation procedures have been extensively applied to power system analysis, particularly to stability analysis of large power systems [26].

During normal steady-state operation, the wind farm can be considered as a PQ node or a PV node depending on the control strategy that the wind farm adopted [27]. In this paper, we assume that the wind farm system is to realize the maximum power tracking through the mechanical control on the wind turbine blade pitch angle and the electrical control on the power converter [28]. Thus the active power output of the aggregated model of the wind farm is determined by $P_{wt}\times N_{wt}$, where N_{wt} is the number of wind turbines in the wind farm. Besides, in the case of one-machine equivalent, the wind farm is reactive-neutral with the entire transmission system in the connection point [26]. This implies that there is no reactive power exchange between the wind farm and the transmission system, with the control of reactive power in the wind farm. With the features of maximum active power tracking and reactive-neutral control, the wind farm embedded in the power system is considered as a PQ node as for power flow calculation.

2.2. Multi-objective optimal dispatch problem

The optimal dispatch problem presented here is to reduce the cost and enhance the voltage stability simultaneously, by optimizing control variables while satisfying a set of operational and physical constraints. It can be formulated as follows:

$$\begin{aligned}&\min\ F(X,U)=[f_1(X,U),f_2(X,U)]\\ &\text{s.t. } g(X,U)=0;\quad h(X,U)\leq 0.\end{aligned} \tag{3}$$

where g and h denote constraints [29]; X and U are control variables and dependant variables respectively, which will be explained in this subsection.

The first objective function, f_1, takes economical and environmental concerns into consideration. It is the sum of fuel cost and the cost of pollutant emission [7]:

$$f_1=\sum_{i=1}^{N_{FG}}f_i'+h\sum_{i=1}^{N_{FG}}E_i \tag{4}$$

where N_{FG} represents the set of numbers of buses incorporated with fuel generators; h is price penalty factor for the emission of atmospheric pollutants, and this factor can be set to the ratio between the maximum fuel cost and the maximum emission of corresponding generator [30]; f_i' and E_i are the fuel cost ($/h) and the amount of

pollutant emission (ton/h) of the ith generator respectively. f_i' can be formulated as:

$$f\prime_i = a_i + b_i P_{G_i} + c_i P_{G_i}^2 \tag{5}$$

where a_i, b_i and c_i are fuel cost coefficients. E_i can be described as follows:

$$E_i = 10^{-2}(\alpha_i + \beta_i P_{G_i} + \gamma_i P_{G_i}^2) + \zeta_i \exp(\lambda_i P_{G_i}) \tag{6}$$

where α_i, β_i, γ_i, ζ_i and λ_i are the coefficients of the ith generator's emission characteristics [7], and P_{G_i} is the real power output generated by the ith generator.

Voltage stability is assessed by a global indicator L_{max}, which expresses the risk of a voltage collapse [31]. It is defined as the maximum value of L-index, which is the stability indicator at every bus of the system, as given in the following [32]:

$$f_2 = L_{max} = \max\{L_j, j = 1, \ldots, N_L\} \tag{7}$$

where L_j is the stability indicator at bus j.

Parameter X in (3) denotes a set of control variables to be optimized, including fuel-derived real power outputs P_G (with the exception of the slack bus, P_{G1}), generator voltages V_G, transformer tap settings T_i and reactive power generations of the capacitor bank Q_{Ci}. Thus, X can be expressed as follows:

$$X = \{P_{Gi} : i \in N_G, i \neq 1\} \cup \{V_{Gj} : j \in N_G\} \cup \{T_k : k \in N_T\} \cup \{Q_{Cl} : l \in N_C\} \tag{8}$$

where N_G represents the set of numbers of generator buses; N_T denotes the set of numbers of transformer branches; and N_C represents the set of numbers of possible installation buses for reactive power sources.

Apart from these control variables, there are still so-called dependent variables, including generator real power outputs at slack bus P_{G1}, load bus voltages V_L, generator reactive power outputs Q_G and apparent power flow S. These dependent variables can be denoted by a vector U, which is expressed as follows:

$$U = P_{G1} \cup \{V_{L_i} : i \in N_L\} \cup \{Q_{Gj} : j \in N_G\} \cup \{S_k : k \in N_E\} \tag{9}$$

where N_E is the set of numbers of transmission lines in the system. Dependent variables U can be obtained through power flow calculation, which adopts Newton–Raphson method to solve the equality constraints of the power systems, which are formulated as nonlinear power flow equations:

$$P_{G_i} = P_{D_i} + V_i \sum_{j \in N_i} V_j (G_{ij} \cos\theta_{ij} + B_{ij} \sin\theta_{ij}) \tag{10}$$

$$Q_{G_i} = Q_{Di} + V_i \sum_{j \in N_i} V_j (G_{ij} \sin\theta_{ij} - B_{ij} \cos\theta_{ij}) \tag{11}$$

where P_{D_i} and Q_{D_i} are demanded real and reactive power at bus i, respectively; G and B are the real and imaginary part of the admittance matrix of the system, respectively; N_i is the set of numbers of buses adjacent to bus i (including bus i). These equality constraints require that the input and output of the real power and reactive power should be equal at each bus [33].

In addition, the dependent variables should satisfy inequality constraints:

$$\begin{aligned}
&P_{G_i}^{min} \leqslant P_{G_i} \leqslant P_{G_i^{max}} \quad i \in N_G \\
&Q_{G_i}^{min} \leqslant Q_{G_i} \leqslant Q_{G_i}^{max} \quad i \in N_G \\
&V_{G_i}^{min} \leqslant V_{G_i} \leqslant V_{G_i}^{max} \quad i \in N_G \\
&V_{L_i}^{min} \leqslant V_{L_i} \leqslant V_{L_i}^{max} \quad i \in N_L \\
&|S_i| \leqslant S_i^{max} \quad i \in N_E \\
&T_i^{min} \leqslant T_i \leqslant T_i^{max} \quad i \in N_T \\
&Q_{C_i}^{min} \leqslant Q_{C_i} \leqslant Q_{C_i}^{max} \quad i \in N_C
\end{aligned} \tag{12}$$

The constraints of the control variables, V_{G_i} and Q_{G_i}, can be satisfied if the search range is defined during the process of optimization. The tap position of transformer T and the amount of reactive power source installation Q_C are self-constrained [29]. In addition, the independent variables should also satisfy inequality constraints. The independent variables are taken into consideration by adding a penalty function, with the inclusion of the penalty factors. This method is commonly used for transforming a constrained optimization problem into an unconstrained one [33]. For instance, the constraints of V_{L_i} is included in the objective function using a penalty factor, λ_V. Then the objective function can be extended as follows:

$$F \leftarrow F + \sum_{i \in N_V^{lim}} \lambda_{V_i} (V_i - V_i^{lim})^2 \tag{13}$$

where V_i^{lim} is defined as:

$$V_i^{lim} = \begin{cases} V_i^{max} & V_i > V_i^{max} \\ V_i^{min} & V_i < V_i^{min} \end{cases} \tag{14}$$

This way of constraining V_{L_i} also holds true for limiting Q_{G_i} and S_i, whose constraints are included in the objective function using penalty factors, λ_Q and λ_S respectively.

3. MOLA

Learning automata methods are well-known with their ability of learning an unknown environment [16,34,17]. Learning automata have been successfully employed in many difficult learning situations over the years [35,36]. It has been noticed that the application of learning automata for optimization, in the area of power systems, has not been attempted. This paper presents multi-objective optimization by learning automata (MOLA) to solve the problem presented in Section 2. The detailed background of the algorithm development can refer to references [33,37,38].

MOLA consists of N automata, where N is equal to the number of dimensions of the solution domain concerned in an optimization problem. In MOLA, $F(X)$ is an N-dimensional function minimization problem to be resolved subject to constraints applied to $F(\cdot)$ or/and X, where $F(\cdot)$ is composed of multiple objective functions, *i.e.* $F(X) = [f_1(X), f_2(X), \ldots, f_m(X)]$, and X is a solution in the N-dimensional space, denoted by $X = [x_1, \ldots, x_i, \ldots, x_N]$, where x_i is the dimensional state of dimension i. Note that X is the combination of N dimensional states and denotes the state of all automata, thus it is also called a state. Each dimension is divided into D cells, and each consists of all the dimensional states located in the cell. Each cell is denoted as $c_{i,j}$, where $i \in \{1, 2, \ldots, N\}$, $j \in \{1, 2, \ldots, D\}$. The width of a cell in the ith dimension is denoted by $w_{c,i}$ and $w_{c,i} = [x_{max,i} - x_{min,i}]/D$. Each cell $c_{i,j}$ has its cell value, denoted as $V(x_i)|_{x_i \in c_{i,j}}$.

3.1. An automaton and its reinforcement scheme

3.1.1. Path value

Before a search action is taken, a possible path is selected to estimate the potential of finding a better solution if MOLA searches down on the path from a dimensional state. Two estimated path values, denoted by $L_l(x_i), l = 1, 2$, are to be found with respect to dimensional state x_i, for selecting one of two possible directions: moving on the left path or on the right path. The value of a path can be estimated as follows:

$$L_l(x_i) = (1 - \lambda_1) \sum_{m=1}^{k-1} \lambda_1^{m-1} v_m^* + \lambda_1^{k-1} v_k^* \quad l = 1, 2 \tag{15}$$

where l denotes the index of the path, k is a pre-set integer, and $v_{l,m}^*$ denotes the mth element of the vector in which the k cell values

$(V(x_i)|_{x_i\in c_{i,j-1}}, V(x_i)|_{x_i\in c_{i,j-2}}, \ldots, V(x_i)|_{x_i\in c_{i,j-k}})$ situated on path l are reordered in descending order.

3.1.2. Action selection

Action selection employs two probabilities, p_1 and p_2. The former is used to select a path which the current dimensional state moves to, while the latter is applied to select the cell on the selected path.

With the availability of the path values, the left path L_1 or the right path L_2 is chosen with a probability given as follows:

$$p_1(L_l(x_i)) = \frac{e^{L_l(x_i)/\tau}}{\sum_{s=1}^{2} e^{L_s(x_i)/\tau}} \quad l = 1,2 \tag{16}$$

Suppose one path is selected. Then a cell, which the current dimensional state moves to, is selected from the k cells located on the path, according to the probability that is calculated from the cell values of the k cells as follows:

$$p_2(V(x_i)|_{x_i\in c_{i,j+s}}) = \frac{e^{V(x_i)|_{x_i\in c_{i,j+s}}/(2\tau)}}{\sum_{z=1}^{k} e^{V(x_i)|_{x_i\in c_{i,j+z}}/(2\tau)}} \tag{17}$$

where $s = 1,2,\ldots,k$. After the cell is chosen, an action is taken by moving from the current dimensional state to a random point of the selected cell. The step length can be denoted as η, $\eta = (\xi+\zeta)w_{c,i}$, where ξ denotes the distance (in the form of number of cells) between the current cell and the selected cell; ζ is a random number and $\zeta \in (0,1]$. With this step length, current dimensional state x_i moves to a new point of the dimension, x_i'.

3.1.3. Reinforcement signal

In order to evaluate the effectiveness of the selected action, it is necessary to observe the reinforcement signal of the search action. Once dimensional state x_i moves to x_i', the ith element of the current state, $X(x_i)$ is replaced by $X(x_i')$. Then a reinforcement signal is assigned to cell $c_{i,j}$ by comparing $X(x_i')$ with the non-dominated solutions found so far in the learning process, according to the following rule:

$$r(X(x_i')) = \begin{cases} 1 & \text{if } X(x_i') \text{ is non-dominated} \\ 0 & \text{otherwise} \end{cases} \tag{18}$$

3.1.4. Evaluation of cell values

As one of the major functions of memory, the value of cell $c_{i,j}$, where the current dimensional state x_i locates, is updated as follows:

$$\begin{aligned} V(x_i)|_{x_i\in c_{i,j}} \leftarrow\ & r(X(x_i)) + \alpha V(x_i)|_{x_i\in c_{i,j}} \\ & + (1-\alpha)((1-\lambda_2)L_{\max}(x_i) + \lambda_2 L_{\min}(x_i)) \end{aligned} \tag{19}$$

where $L_{\max}(x_i)$ and $L_{\min}(x_i)$ are the two estimated path values at dimensional state x_i, while satisfying $L_{\max}(x_i) = \max\{L_1(x_i), L_2(x_i)\}$ and $L_{\min}(x_i) = \min\{L_1(x_i), L_2(x_i)\}$.

3.1.5. Forming the Pareto set

The non-dominated solutions found in the optimization process are stored in an elite list, denoted as $\mathbb{L}$. Suppose the state moves from $X(x_i)$ to $X(x_i')$, if $X(x_i')$ is not dominated by the solutions that were stored in $\mathbb{L}$ previously, it will be denoted as X_{best}. The relationship between X and X_{best} can be described by the following rule:

$$X_{\text{best}} \leftarrow \begin{cases} X(x_i') & \text{if } X(x_i') \text{ is non-dominated} \\ X_{\text{best}} & \text{otherwise} \end{cases} \tag{20}$$

where $X(x_i') = [x_1,\ldots,x_{i-1},x_i',x_{i+1},\ldots,x_N]$. Then $\mathbb{L}$ is updated based on the following rule:

$$\mathbb{L} \leftarrow \begin{cases} \mathbb{L}\cup\{X_{\text{best}}\} - B & \text{if } r = 1 \\ \mathbb{L} & \text{otherwise} \end{cases} \tag{21}$$

where B is a set of the solutions which were previously stored in the elite list but are currently dominated by X_{best}, as formulated in the following equation:

$$B = \{X : X \in \mathbb{L}, F(X) \succeq F(X_{\text{best}})\} \tag{22}$$

3.2. Learning from neighborhood

Suppose current state X is one of the non-dominated solutions stored in elite list $\mathbb{L}$. It is believed that the neighboring solutions of X carry more useful information that can benefit the search around X, and they can make more contributions than that of the remote solutions [11]. To find out the relationship among the non-dominated solutions, an uniform spread of M weight vectors, $(\mathbf{W}^1,\ldots,\mathbf{W}^i,\ldots,\mathbf{W}^M)$, where $\mathbf{W}^i = [w_1,w_2,\ldots,w_m]$ and $\sum(\mathbf{W}) = 1$, are initialized at the beginning of the learning process [11]. Then the Euclidean distances between any two weight vectors are calculated, and the $M/4$ closest weight vectors to each weight vector can be found regarding the Euclidean distances. Let the indexes of the $M/4$ closest weight vectors to $\mathbf{W}^i$ be denoted as set $D(i)$.

Each weight vector, $\mathbf{W}^i$ $(i = 1,2,\ldots,M)$, is associated with a subsolution, denoted as X^i_{sub}, which is selected from the elite list according to Tchebycheff rule as follows:

$$X^i_{\text{sub}} = \text{argmin}_{X\in\mathbb{L}} g^{\text{te}}(X|\mathbf{W}^i, z^*) \tag{23}$$

where Tchebycheff value $g^{\text{te}}(X|\mathbf{W}^i,z^*)$ is defined as [39]

$$g^{\text{te}}(X|\mathbf{W}^i,z^*) = \max_{1\leqslant j\leqslant \text{mf}}\left\{w_j\frac{|f_j(X)-z_j^*|}{f_{j,\text{range}}}\right\},$$

and $z^* = (z_1^*,\ldots,z_j^*,\ldots,z_m^*)$ is the reference point, *i.e.* $z_j^* = \min\{f_j(X)|X\in\mathbb{L}\}$; $f_{j,\text{range}}$ is the estimated range of f_j, *i.e.* $f_{j,\text{range}} = \max\{f_j(Y)|Y\in\mathbb{L}\} - \min\{f_j(X)|X\in\mathbb{L}\}$.

After each weight vector is assigned with a subsolution, the neighboring solutions of X^i_{sub} include the subsolutions that are corresponding to the weight vectors of set $D(i)$. The set of the neighboring solutions of X^i_{sub} is denoted as set $\text{Nei}(X^i_{\text{sub}})$, and it can be formulated as:

$$\text{Nei}(X^i_{\text{sub}}) = \{X^j_{\text{sub}} | j \in D(i)\} \tag{24}$$

With the neighborhood introduced above, each subsolution X^i_{sub} is updated based on its neighboring solutions. Two indexes, r_1 and r_2, will be randomly selected from $D(i)$, and a new solution can be generated according to the following learning operation:

$$\bar{y} = X^i_{\text{sub}} + 0.5\times(X^{r_1}_{\text{sub}} - X^{r_2}_{\text{sub}}) \tag{25}$$

Then $\bar{y}$ will be used to replace X^i_{sub} if its Tchebycheff value is smaller than that of X^i_{sub}. Simultaneously, $\bar{y}$ will be used to update X_{best} and $\mathbb{L}$ according to (20) and (21) respectively if it is not dominated by the solutions that are stored in $\mathbb{L}$.

3.3. Perturbation operation

To increase the diversity and fully explore the probability of finding the Pareto set, different perturbations are introduced to the non-dominated solutions stored in the elite list, except for the solutions that have been selected as subsolutions in the process of learning operation. The members of the elite list are updated as follows:

$$X \leftarrow X + \Delta + \beta(X_{\text{best}} - X) \tag{26}$$

where $\Delta_i = \text{sign}(\kappa)\zeta(x_{\max,i} - x_{\min,i})$, ζ is a random variable and $\zeta \in [0,\frac{k}{D}]$. The sign function is used to choose the moving direction

of x_i. Suppose x_i is located in cell $c_{i,j}$, then the input to the sign function is the subtraction of the two adjacent cell values of $c_{i,j}$. Once completing the operation, X_{best} and $\mathbb{L}$ are updated according to (20) and (21) respectively.

3.4. The implementation of MOLA

Starting with the first state X, at dimensional state x_i, a search is undertaken by calculating path values (15), and taking an action according to (16) and (17). A reinforcement signal is generated according to (18). Then the cell value of $c_{i,j}$, in which dimensional state x_i locates, is updated using (19). X_{best} and $\mathbb{L}$ are updated according to (20) and (21) respectively. If the reinforcement signal is not equal to 1, the current iteration ends and the next automaton is selected in order for MOLA computation to continue. Otherwise searching on this path is regarded worthy, and the search action is taken continuously for I_{emax} times in the same way presented in (15)–(21). An iteration completes after the exploitation, which has updated X_{best} and all values of the cells visited, before the next automaton is selected. All automata are selected sequentially once, followed by the learning operation and perturbation operation. The aforementioned process is called one episode. The MOLA computation proceeds in episodes, until a given maximum number of function evaluations, N_{femax}, is reached.

4. Simulation studies

MOLA is fully compared with MOEA/D [11,22] and NSGA-II [12], based on the modified midwestern American electric power system and IEEE 118-bus test system, which are penetrated with wind power. The parameters setting of MOEA/D and NSGA-II follows the suggestions in [11,12] respectively. The parameters of MOLA do not affect the performance substantially when MOLA is applied to solve different optimization problems, and they are chosen empirically and preset as follows: $\alpha = 0.8$; $\tau = 0.2$; $k = 4$; $I_{emax} = 5$; $\lambda_1 = 0.5$; $\lambda_2 = 0.25$; $M = 50$; $D = 15$. To compare the algorithms fairly, the same N_{femax} is taken by the three algorithms when solving the same test case. The coefficients in (6) follow the suggestions given in [7].

The problem aims to gain a set of non-dominated solutions whose objective function vectors are evenly distributed on the Pareto front. The quality of the Pareto front is evaluated by the hypervolume indicator (denoted as *HV*), which is a measure used in evolutionary multiobjective optimization to evaluate the performance of search algorithms [40]. Given a reference point, *HV* is the volume (in objective function space) covered by the non-dominated solutions of the problems in which all objectives are to be minimized [41]. The property of this performance indicator is that it measures both convergence to the true Pareto front and diversity of the obtained fronts. Higher values of this performance indicator imply more desirable solutions and wider Pareto front obtained.

4.1. Modified midwestern American electric power system

The modified midwestern American electric power system (*i.e.* IEEE bus-30 test system) consists of 41 branches and 6 fuel generators. Nodes 7, 10, 16, 24 and 30 are incorporated with wind farms.

4.1.1. Static environment

The wind speed and number of wind turbines operated in the wind farms are given in Table 1. The rated power of all wind farms is 80 MW, and the rated power of fuel generators is 435 MW.

Control variables X include generator real power outputs, generator voltages, transformer tap settings and reactive power generations of the capacitor bank. In the application, the setting of N_{femax} should ensure that N_{femax} is large enough for the three algorithms to converge to their own best Pareto fronts. For this power system, N_{femax} is set to 30,000.

The best Pareto fronts obtained by the three algorithms are presented in Fig. 1, which plots the obtained solutions that satisfy the constraints of the problem. It is obvious that MOLA outperforms NSGA-II in terms of finding accurate non-dominated solutions and wide range of the Pareto fronts. The non-dominated solutions obtained by MOEA/D and MOLA overlap in the objective space. However, the range of their Pareto fonts varies widely. The non-dominated solutions found by MOEA/D flock to one end, situating at the range of $[709.483, 709.97] \times [0.1013, 0.1071]$. Among the solutions found by MOEA/D, there is an isolated point, *i.e.* $(709.97, 0.1013)$. Besides, a big gap exists between solutions $(709.66, 0.1027)$ and $(709.97, 0.1013)$, which implies that MOEA/D has difficulty in finding the solutions located in the gap. As for MOLA, its non-dominated solutions spread over the range of $[709.437, 721.524] \times [0.0901, 0.1071]$, which is much wider than that of MOEA/D. Furthermore, the non-dominated solutions found by MOLA dominate the isolated solution obtained by MOEA/D, *i.e.* $(709.97, 0.1013)$. MOLA can find more non-dominated solutions (224) than that of MOEA/D (101). The fact that MOLA finds wider Pareto front and more non-dominated solutions than MOEA/D suggests that MOLA can provide more options of the non-dominated solutions that satisfy the optimization targets. Moreover, the best and compromise solutions shown in Fig. 1, together with the computation time consumed by the three algorithms are provided in Table 2.

The reference solution that is employed to calculate *HV* is $[721.2, 0.108]$. The mean and standard deviation of *HV* obtained by these algorithms over 30 runs are given in Table 3. It can be seen that MOLA outperforms MOEA/D and NSGA-II, as it finds larger *HV* on average. In addition, the standard deviation of *HV* obtained by MOLA is smaller than that obtained by MOEA/D and NSGA-II. This fact presents the reliability of MOLA in solving this problem.

4.1.2. Dynamic environment

The demand for electricity and wind power fluctuate throughout the day in the dynamic environment. Therefore, the economic dispatch problem is essentially a dynamic optimization problem, which requires algorithms to track the trajectory of the changing optima over the dynamic environment [42]. In order to simulate the time-varying operation condition, the whole optimization process proceeds based on the number of Function Evaluations (FEs) applied by the algorithms. In other words, after the optimization algorithm, such as MOLA, applies a certain number of FEs, different load demand and wind speed are provided for the power system. In this case, the number of FEs allowed under one operation condition (called a stage) is set to 20,000, which is large enough for the algorithms to converge before the new operation condition occurs. The fluctuating load demand is given in Table 4. Nodes 7, 10, 16, 24 and 30 are incorporated with wind farms, and wind speeds of these locations are given in Table 5. NSGA-II, MOEA/D and MOLA are applied to solve the multi-objective problem in this power system to prove their tracking abilities. The algorithm with better tracking ability means that it can find the changing optima rapidly and accurately in the dynamic power system.

Table 1
Wind speed and number of wind turbines in the wind farms.

Node	7	10	16	24	30
Wind speed (m/s)	9.3	15	7.6	8.7	6.5
Number of turbines	10	5	10	5	10

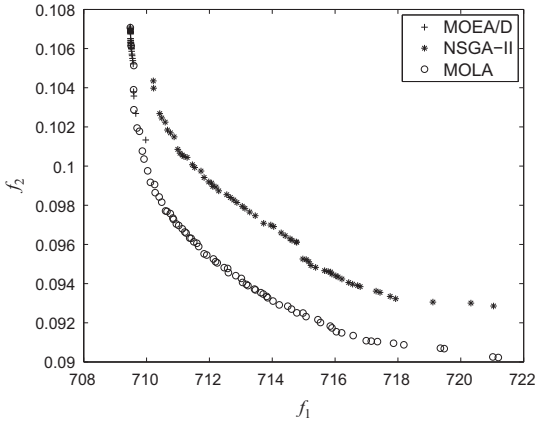

Fig. 1. Pareto fronts obtained by MOEA/D, NSGA-II and MOLA on the midwestern American wind power penetrated system.

Fig. 2 shows the hypervolume convergence characteristics obtained by the three algorithms, the reference point is set to be (700, 0.1). It should be mentioned that the setting of penalty factors given in (13) is relevant to this reference point. In the paper, the penalty factors are set to 100 × (f_1 of the reference point). With this setting, the solutions which are outside of the constraints will have large fitness values which are more likely to go beyond the reference point. These solutions are regarded as unqualified ones and not used to calculate the hypervolume. Besides, to avoid the existence of small violations among the obtained solutions, only the solutions which satisfy the constraints of the problem are considered as qualified ones. Notice that the higher the hypervolume values are, the better the Pareto front is. For simplicity, the optimization process of one operation condition is called one stage. It can be seen from Fig. 2 that between two stages, there is a sharp drop of the hypervolume values. This is because at the beginning of a new stage, the power demand and wind power change, and the objective function vectors need to be newly recorded. Besides, some of the non-dominated solutions obtained in the previous stage are not qualified as non-dominated solutions any more, and they are not suitable for the new operation condition. With the exploration strategies employed by the algorithms, the hypervolume values could be very small at the beginning of one stage until a larger hypervolume value is found. Among the three algorithms, MOEA/D and NSGA-II have a more serious drop of hypervolume values when power demand and wind power vary, which implies that the previously obtained solutions provide less inheritable information for the new stage, in terms of finding non-dominated solutions which are suitable for the new operation condition. It can be seen from Fig. 2 that MOLA has a faster converge rate in the first stage, compared with MOEA/D and NSGA-II. For the

Table 3
HV obtained by NSGA-II, MOEA/D and MOLA on the modified midwestern American electric power system.

	MOEA/D	NSGA-II	MOLA
Mean	0.0770	0.1327	0.1714
Std	0.0041	0.0075	0.0027

Table 4
Load demand (MW) at Bus 10.

FEs (10,000×)	0–2	2–4	4–6	6–8	8–10	10–12
Load demand	2.5	3.5	5.5	4.7	5	3.8

Table 2
The best and compromise solutions shown in Fig. 1.

	Best f_1	Best f_2	Best compromise (MOEA/D)	Best compromise (NSGA-II)	Best compromise (MOLA)
P_{G_1}	159.7981	140.7317	156.9994	166.3565	145.7724
P_{G_2}	44.6087	49.5747	48.6675	51.9970	44.4588
P_{G_5}	18.7759	20.0138	18.9142	22.3237	20.1453
P_{G_8}	16.4278	24.7763	13.0424	20.8208	22.6316
$P_{G_{11}}$	11.7545	15.6591	13.5482	13.9816	16.4821
$P_{G_{13}}$	13.5703	15.0365	13.6110	14.1610	14.3016
V_{G_1}	0.9986	1.0069	1.0108	0.9931	1.0015
V_{G_2}	0.9856	1.0011	0.9996	0.9762	0.9886
V_{G_5}	0.9667	0.9656	0.9733	0.9648	0.9657
V_{G_8}	0.9668	0.9892	0.9834	0.9698	0.9767
$V_{G_{11}}$	1.0749	1.0618	1.0752	1.0652	1.0615
$V_{G_{13}}$	1.0476	1.0602	1.0582	1.0489	1.0536
T_{11}	1.0000	0.9750	1.0000	0.9500	0.9625
T_{12}	0.9625	1.0000	0.9875	0.9625	1.125
T_{15}	0.9750	0.9625	0.9750	0.9750	0.9875
T_{36}	0.9750	1.0000	0.9625	1.125	0.9625
$Q_{C_{10}}$	0.01	0.04	0.03	0.03	0.02
$Q_{C_{12}}$	0.02	0.02	0.02	0.02	0.02
$Q_{C_{15}}$	0.01	0.05	0.01	0.05	0.05
$Q_{C_{17}}$	0.02	0.02	0.04	0.02	0.02
$Q_{C_{20}}$	0.03	0.04	0.01	0.03	0.03
$Q_{C_{21}}$	0.02	0.02	0.03	0.03	0.05
$Q_{C_{23}}$	0.04	0.04	0.01	0.05	0.02
$Q_{C_{24}}$	0.02	0.01	0.03	0.02	0.03
$Q_{C_{29}}$	0.03	0.01	0.03	0.03	0.05
Fuel cost ($/h)	708.7259	720.0557	708.8288	712.5179	711.2151
Emission (ton/h)	0.3269	0.2884	0.3211	0.2891	0.2969
f_1	709.4365	721.2536	709.5269	713.1462	711.8605
f_2	0.1071	0.0901	0.1057	0.981	0.0958
Computation time (s)	332.297	332.297	424.980	373.981	332.297

Table 5
Wind speed in midwestern American electric power system.

FEs (10,000×)	0–2	2–4	4–6	6–8	8–10	10–12
7	5.6	7.3	10.1	12.7	9.4	10.5
10	10.3	8.6	6.7	5.6	7.1	9.0
16	9.7	10.9	12.6	9.8	8.4	6.9
24	8.4	11.3	10.7	8.6	10.3	9.3
30	17	12.3	10.6	9.4	7.9	10.3

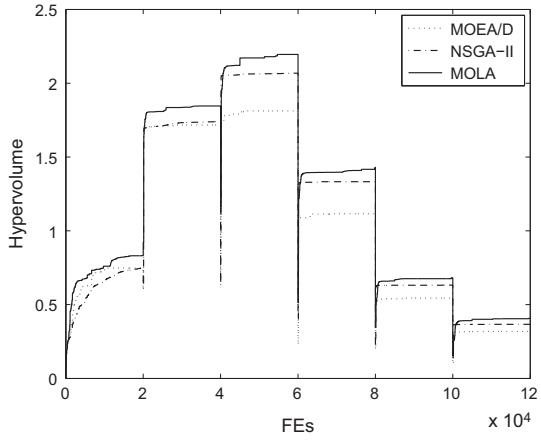

Fig. 2. Convergence characteristics of MOEA/D, NSGA-II and MOLA on the midwestern American electric power system with wind power penetration.

following stages, MOLA is able to track the changes of the power demand and wind power more accurately than the other two algorithms, and the hypervolume values obtained by MOLA are larger than those obtained by MOEA/D and NSGA-II. As for MOEA/D, its hypervolume values increase faster than that of NSGA-II in the first stage, and has similar performance as NSGA-II in the second stage. However, the performance of MOEA/D is much worse than that of NSGA-II in stages 3–6. As for NSGA-II, its convergence curve is almost flat within one stage (with the exception of stage 1). This implies that its search strategy applied to stages 2–6 does not take significant effect after the first change of the operation condition.

In addition, the minimal objective function values obtained by these algorithms in different stages are given in Table 6, and the corresponding solutions of f_1 are also presented in Table 7. It can be seen that MOLA outperforms MOEA/D and NSGA-II under different operation conditions, as it can find both smaller cost and index of voltage stability.

4.2. IEEE 118-bus test system

The standard IEEE 118-bus power system is used as a test case in the simulation. The system consists of 186 branches and 54 fuel generators, nodes 11, 45, 60, 78, 82 and 88 are incorporated with wind farms.

4.2.1. Static environment

The wind speed and number of wind turbines operated in the wind farms are given in Table 8. The rated power of all wind farms is 1250 MW, and the rated power of fuel generators is 6699 MW. N_{femax} is set to 150,000 for MOEA/D, NSGA-II and MOLA.

The Pareto fronts obtained by the algorithms are given in Fig. 3. It can be seen that MOLA greatly presents its superiority over MOEA/D and NSGA-II with respect to the following fact: the non-dominated solutions found by MOLA are more convergenced than those found by MOEA/D and NSGA-II, *i.e.* the solutions obtained by MOLA dominate those obtained by MOEA/D and NSGA-II. Moreover, the total cost, total emission of the compromise solution, and the execution time in terms of MOEA/D, NSGA-II and MOLA are given in Table 9. It shows that MOLA can find better compromise solution [7] while consuming less computation time.

4.2.2. Dynamic environment

NSGA-II, MOEA/D and MOLA are applied to solve the multi-objective problem in the IEEE 118-bus system that is embedded with fluctuating power demand and wind power, which vary once a certain number of FEs has been applied by the algorithms. The power demand of different stages is given in Table 4. The wind speed at nodes 11, 45, 60, 78, 82 and 88 varies according to Table 10, in which $\tilde{v}$ denotes the random values generated according to a Rayleigh distribution $f(\tilde{v}) = \frac{\tilde{v}-0.2}{\sigma^2} e^{-(\tilde{v}-0.2)^2/2\sigma^2}$ whose parameter σ is set to 0.2 [43]. In this case, the uncertainty of the wind speed is simulated by adding a random value to the scheduled wind speed at each function evaluation. Each algorithm is allowed to perform 100,000 FEs under one operation condition. Ramp rate limits of generators are considered by composing the change rate of real power outputs applied in a certain time interval within a specified range. To fulfill this constraints in a simple way, both ramp up and ramp down of generates are set to 10% of the maximum capacity of the power generators. The cost of the wind generation, C_{W}, is considered and added in the objective function f_1. C_{W} is defined as follows [43]:

$$C_{\text{W}} = K_L \cdot \Pr(P_{\text{W}} < P_{\text{s}}) \cdot (P_{\text{s}} - E_{P_{\text{W}}<P_{\text{s}}}(P_{\text{W}})) + K_H \cdot \Pr(P_{\text{W}} > P_{\text{s}}) \cdot (E_{P_{\text{W}}>P_{\text{s}}}(P_{\text{W}}) - (P_{\text{s}}) \quad (27)$$

where P_s is the scheduled wind power output which is calculated from the scheduled wind speed provided in Table 10; P_{WF} is the actual wind power output; $\Pr(P_{\text{W}} < P_{\text{s}})$ and $\Pr(P_{\text{W}} > P_{\text{s}})$ are the probabilities of wind power shortage occurrence and remnant occurrence respectively; E is the expectation of wind power output under a specified condition; K_L and K_H are two coefficients which are set to 0.01 and 0.02 respectively.

Fig. 4 shows the convergence of the obtained hypervolume values, while the reference point is set to (7E12, 0.1). It can be observed that the tracking ability of MOLA is consistently better

Table 6
The minimum objective function values.

	Min f_1	Min f_2	Min f_1	Min f_2	Min f_1	Min f_2
	1–20,000 FEs		20,001–40,000 FEs		40,001–60,000 FEs	
MOEA/D	670.958	0.0778	641.894	0.0723	631.088	0.0753
NSGA-II	684.219	0.0796	642.966	0.0696	631.465	0.0701
MOLA	0.8670.669	0.8 0.0708	0.8641.758	0.80.0675	0.8631.062	0.8 0.0681
	60,001–80,000 FEs		80,001–100,000 FEs		100,001–120,000 FEs	
MOEA/D	646.238	0.0831	674.100	0.0772	683.570	0.0825
NSGA-II	646.744	0.0761	675.098	0.0753	684.639	0.0757
MOLA	0.8645.342	0.8 0.0739	0.8673.959	0.8 0.0733	0.8683.508	0.8 0.0742

Table 7
The solutions of f_1 as for Scenarios 1–6.

	Scenario 1	Scenario 2	Scenario 3	Scenario 4	Scenario 5	Scenario 6	Min	Max
P_{G_1}	154.1484	148.3956	147.013	143.2931	155.9229	156.6977	50	200
P_{G_2}	43.1447	42.4553	41.8508	41.8099	44.3022	44.2231	20	80
P_{G_5}	18.3541	19.3595	19.6467	16.0660	20.1968	19.9152	15	50
P_{G_8}	12.7841	11.4202	10.4468	16.0980	11.6393	13.2781	10	35
$P_{G_{11}}$	11.9562	10.2647	10.1709	13.7434	10.2570	11.1036	10	30
$P_{G_{13}}$	12.8664	12.5155	12.0288	13.4093	12.2002	12.1110	12	40
V_{G_1}	1.0087	1.0474	1.0099	1.0097	1.0065	1.0192	0.95	1.10
V_{G_2}	0.9952	1.0374	1.0365	1.0333	1.0331	1.0047	0.95	1.10
V_{G_5}	0.9781	1.0099	1.0085	1.0034	1.0033	1.1521	0.95	1.10
V_{G_8}	1.0683	1.0172	1.0170	1.0102	1.0091	0.9870	0.95	1.10
$V_{G_{11}}$	1.0180	1.0781	1.0799	1.0867	1.0912	0.9921	0.95	1.10
$V_{G_{13}}$	1.0641	1.0743	1.0645	1.0627	1.0684	1.0758	0.95	1.10
T_{11}	0.9250	1.0000	0.9875	0.9875	0.9875	1.0675	0.90	1.10
T_{12}	0.9625	0.9625	0.9625	0.9500	0.9625	0.9875	0.90	1.10
T_{15}	0.9250	1.0000	0.9875	0.9750	0.9875	0.9625	0.90	1.10
T_{36}	0.9750	0.9500	0.9625	0.9500	0.9500	1.0000	0.90	1.10
$Q_{C_{10}}$	0.03	0.05	0.05	0.03	0.02	0.03	0.00	0.05
$Q_{C_{12}}$	0.03	0.02	0.05	0.03	0.05	0.04	0.00	0.05
$Q_{C_{15}}$	0.04	0.03	0.05	0.04	0.03	0.05	0.00	0.05
$Q_{C_{17}}$	0.02	0.05	0.05	0.05	0.05	0.03	0.00	0.05
$Q_{C_{20}}$	0.05	0.04	0.04	0.05	0.04	0.02	0.00	0.05
$Q_{C_{21}}$	0.03	0.05	0.05	0.05	0.05	0.04	0.00	0.05
$Q_{C_{23}}$	0.00	0.03	0.02	0.03	0.04	0.05	0.00	0.05
$Q_{C_{24}}$	0.04	0.05	0.05	0.05	0.05	0.04	0.00	0.05
$Q_{C_{29}}$	0.02	0.02	0.03	0.03	0.03	0.03	0.00	0.05
Fuel cost ($/h)	669.9799	641.0906	630.3990	644.6960	673.2611	682.8088		
Emission (ton/h)	0.3168	0.3071	0.3050	0.2968	0.3208	0.3218		

Table 8
Wind speed and number of wind turbines in the wind farms.

Node	11	45	60	78	82	88
Wind speed (m/s)	8.4	10.9	10.5	9.7	9.4	11.5
Number of turbines	100	150	100	100	125	50

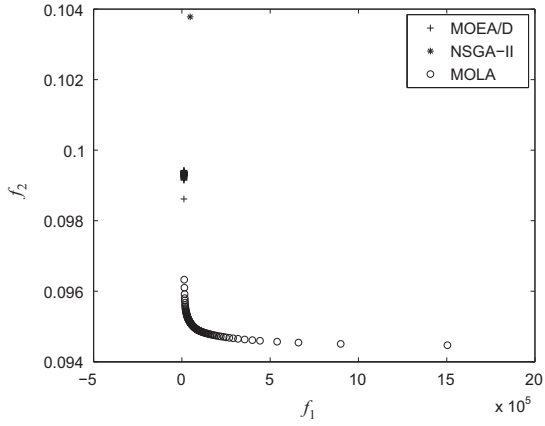

Fig. 3. Pareto fronts obtained by MOEA/D, NSGA-II and MOLA on the IEEE 118-bus system wind wind power penetration.

Table 9
Results of the wind power penetrated IEEE 118-bus system.

	MOEA/D	NSGA-II	MOLA
Total cost ($/h)	101370.1	101372.6	101362.5
Total emission (ton/h)	29.56	30.21	28.94
Computation time (s)	4832.0	4255.6	3356.5

Table 10
Wind speed on the wind power penetrated IEEE 118-bus system (scheduled wind speed + uncertainty).

FEs (100,000×)	0–1	1–2	2–3	3–4	4–5	5–6
11	$7.9+\tilde{v}$	$7.4+\tilde{v}$	$6.7+\tilde{v}$	$5.7+\tilde{v}$	$4.5+\tilde{v}$	$5.6+\tilde{v}$
45	$10.4+\tilde{v}$	$9.5+\tilde{v}$	$10.3+\tilde{v}$	$9.7+\tilde{v}$	$7.8+\tilde{v}$	$7.3+\tilde{v}$
60	$10+\tilde{v}$	$11.3+\tilde{v}$	$8.4+\tilde{v}$	$7.4+\tilde{v}$	$6.9+\tilde{v}$	$7.9+\tilde{v}$
78	$10.2+\tilde{v}$	$8.6+\tilde{v}$	$5.3+\tilde{v}$	$5.9+\tilde{v}$	$6.3+\tilde{v}$	$5.9+\tilde{v}$
82	$9.8+\tilde{v}$	$8.9+\tilde{v}$	$7.4+\tilde{v}$	$7.1+\tilde{v}$	$7.8+\tilde{v}$	$8.9+\tilde{v}$
88	$11.2+\tilde{v}$	$10.5+\tilde{v}$	$9.9+\tilde{v}$	$9.3+\tilde{v}$	$8.9+\tilde{v}$	$10.4+\tilde{v}$

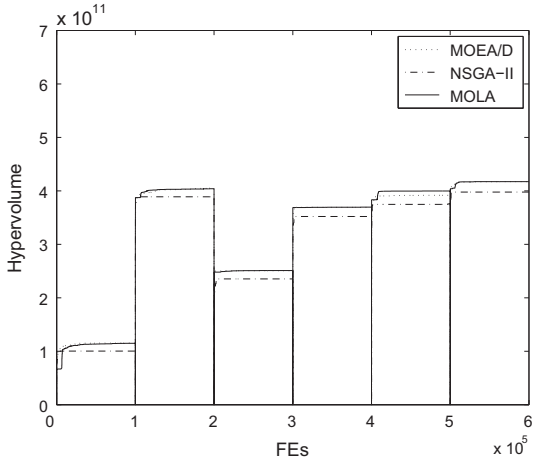

Fig. 4. Convergence characteristics of MOEA/D, NSGA-II and MOLA on the IEEE 118-bus system with wind power penetration.

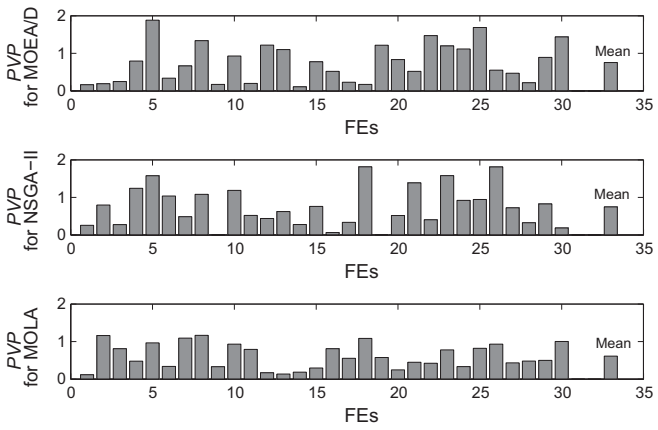

Fig. 5. The values of *PVP* obtained by MOEA/D, NSGA-II and MOLA.

than that of MOEA/D and NSGA-II as the function evaluation proceeds from stages 2–6. The convergence performance of MOLA reveals that the variation of its hypervolume values is in line with the variation of power demand and wind power.For this power system, NSGA-II cannot converge to acceptable solutions.

4.3. Remarking of voltage profile

Unlike MOEA/D and NSGA-II that change all the control variables simultaneously, MOLA mainly applies sequential search, which adjusts control variables one by one. Sequential search has the advantage of avoiding large perturbation of voltage, *i.e.* maintaining the variation of voltage profile in a reasonable range. Keeping voltage profile stable is one of the most important constraints in terms of the implementation of an optimization algorithm in power systems. In the process of optimization, the voltage profile is evaluated through an indicator of the perturbation of the voltage profile, denoted as *PVP*, which is defined as the difference of voltage profile between two continuous function evaluations:

$$PVP_i = \sum_{j\in N} |V_{ij} - V_{i-1j}|, \quad i = 1, 2, \ldots, \mathrm{FEs} \tag{28}$$

where N denotes the set of numbers of the buses in the power system. *PVP* represents the perturbation of the voltage profile between two evaluations in the optimization process. Smaller values of *PVP* imply a stabler voltage profile. The values of *PVP* obtained over 31 continuous power flow calculations are given in Fig. 5, as well as its mean value. The mean value of *PVP* obtained by MOLA is 0.6133, while those of MOEA/D of NSGA-II are 0.7557 and 0.7473 respectively. It can be seen that the voltage profile obtained by MOLA is better than that found by MOEA/D and NSGA-II on average.

5. Conclusion

The multi-objective optimization by learning automata (MOLA) has been applied to optimize two objectives, economic emission dispatching and voltage stability enhancement, in the environment where the wind power and load demand vary. MOLA capitalises on the merits of dimensional learning, state memory and sequential search, which enable MOLA to find accurate solutions and track the variation of wind power and load efficiently, in particular in the case of power system voltage control which needs to avoid large perturbation of the voltage profile. MOLA has been fully compared with MOEA/D and NSGA-II in the modified midwestern American electric power system and IEEE 118-bus test power system respectively, which are penetrated with wind power. The simulation results have demonstrated that MOLA greatly outperforms MOEA/D and NSGA-II, as MOLA can find wider distributed Pareto fronts, obtain more accurate solutions, and track the varying wind power and load demand rapidly and accurately in the dynamic environment.

Acknowledgements

This work was supported by the Guangdong Innovative Research Team Program (No. 201001N0104744201) and the National Key Basic Research and Development Program (973 Program, No. 2012CB215100).

References

[1] Shabanpour-Haghighi A, Seifi AR, Niknam T. A modified teachinglearning based optimization for multi-objective optimal power flow problem. Energy Convers Manage 2014;77:597–607.
[2] Rezaei Adaryani AKM. Artificial bee colony algorithm for solving multi-objective optimal power flow problem. Int J Electr Power Energy Syst 2013;53(3):219–30.
[3] Niknam T, Narimani M, Aghaei J, Azizipanah-Abarghooee R. Improved particle swarm optimisation for multi-objective optimal power flow considering the cost, loss, emission and voltage stability index. IET Gener Transm Distrib 2012;6(6):515–27.
[4] Sivasubramani S, Swarup K. Multi-objective harmony search algorithm for optimal power flow problem. Int J Electr Power Energy Syst 2011;33(3):745–52.
[5] Kuo CC. Generation dispatch under large penetration of wind energy considering emission and economy. Energy Convers Manage 2010;51(1):89–97.
[6] Delarue ED, Luickx PJ, D'haeseleer WD. The actual effect of wind power on overall electricity generation costs and CO_2 emissions. Energy Convers Manage 2009;50(6):1450–6.
[7] Abido MA. Environmental/economic power dispatch using multiobjective evolutionary algorithms. IEEE Trans Power Syst 2003;18(4):1529–37.
[8] Boulaxis NG, Papathanassiou SA, Papadopoulos MP. Wind turbine effect on voltage profile of distribution network. Renew Energy 2002;25(3):401–15.
[9] Technique for voltage stability assessment using newly developed line voltage stability index. Energy Convers Manage 2008;49(2):267–75.
[10] Brini S, Abdallah HH, Ouali A. Economic dispatch for power system included wind and solar thermal energy. Leonardo J Sci 2009;8(14):204–20.
[11] Zhang QF, Li H. MOEA/D: a multiobjective evolutionary algorithm based on decomposition. IEEE Trans Evol Comput 2007;11(6):712–31.
[12] Deb K, Agrawal S, Pratap A, Meyarivan T. A fast and elitist multiobjective genetic algorithm: NSGA-II. IEEE Trans Evol Comput 2002;6(2):182–97.
[13] Konak A, Coit DW, Smith AE. Multi-objective optimization using genetic algorithms: a tutorial. Reliab Eng Syst Saf 2006;91(9):992–1007.
[14] Wu QH, Lu Z, Li MS, Ji TY. Optimal placement of facts devices by a group search optimizer with multiple producers. In: Proc of IEEE Congr on Evolut Comput; 2008. p. 1033–9.
[15] Liao H, Wu Q. Optimal power flow in wind power integrated systems using function optimization by learning automata. Power Energy Soc Gener Meet, 2011 IEEE 2011;33(3):1–8.
[16] Wu Q. Reinforcement learning control using interconnected learning automata. Int J Control 1995;62:1–16.
[17] Lee B, Lee K. Application of S-model learning automata for multi-objective optimal operation of power systems. IEE Proc Gener, Transm Distrib 2005;152:295–300.
[18] Howell M, Gordon T, Brandao F. Genetic learning automata for function optimisation. IEEE Trans Syst, Man, Cyber, Part B: Cyber 2002;32:804–15.
[19] Beigy H, Meybodi M. Stochastic optimisation using continuous action-set learning automata. Sci Iran 2005;12:14–25.
[20] Liao H, Wu Q. Multi-objective optimization by learning automata. J Global Optim 2013;55:459–87.
[21] Karakas A, Kocatepe C, Li F. Using learning automata for multi-objective generation dispatch considering cost, voltage stability and power losses. Turk J Elec Eng Comp Sci 2011;19:913–27.
[22] Special session on performance assessment of multiobjective optimization algorithms/cec 09 moea competition. Tech rep; 2009. <http://dces.essex.ac.uk/staff/qzhang/moeacompetition09.htm>.
[23] Zhou W, Peng Y, Sun H.,Probabilistic wind power penetration of power system using nonlinear predictor-corrector primal-dual interior-point method. In: Proc of the third int conf on electric utility deregulation and restructuring and power technol; 2008.
[24] Conroy J, Watson R. Aggregate modelling of wind farms containing full-converter wind turbine generators with permanent magnet synchronous machines: transient stability studies. IET Renew Power Gener 2009;3(1):39–52.
[25] Shafiu GBA, Anaya-Lara O, Jenkins N. Aggregated wind turbine models for power system dynamic studies. Wind Eng 2006;30(3):171–86.

[26] Akhmatov V. An aggregated model of a large wind farm with variable-speed wind turbines equipped with doubly-fed induction generators. Wind Eng 2004;28(4):479–88.
[27] Patnaik I. Wind as a renewable source of energy. Technical report.
[28] Chen X, Sun H, Wen J, Lee W-J, Yuan X, Li N, et al. Integrating wind farm to the grid using hybrid multiterminal hvdc technology. IEEE Trans Ind Appl 2011;47(2):965–72.
[29] Wu QH, Cao YJ. In: Webster John G, editor. Dispatching, encyclopaedia of electrical and electronics engineering. John Wiley & Sons Inc.; 1999.
[30] Bharathi R, Kumar MJ, Sunitha D, Premalatha S. Optimization of combined economic and emission dispatch problem – a comparative study. In: Proc of IPEC 2007 int power eng conf; 2007. p. 134–9.
[31] Liao HL, Wu QH. Multi-objective optimization by reinforcement learning for power system dispatch and voltage stability. In: Proc of IEEE PES conf on innovative smart grid tech Europe, Sweden; 2010. p. 1–8.
[32] He S, Prempain E, Wu QH, Fitch J, Mann S. An improved particle swarm optimization for optimal power flow. In: Proc of IEEE 2004 int conf on power syst technol, The Pan Pacific, Singapore, vol. F1628-2E2J(1-5); 2004. p. 21–4.
[33] Wu QH, Liao HL. Function optimization by reinforcement learning for power system dispatch and voltage stability. In: Proc of IEEE power energy soc gen meet, Minneapolis, USA; 2010.
[34] Wu Q, Liao H. Function optimisation by learning automata. Inform Sci 2013;220:379–98.
[35] Garcia HE, Ray A, Edwards RM. Reconfigurable control of power plants using learning automata. IEEE Control Syst Mag 1991;11(1):85–922.
[36] Aghaebrahimi MR, Zahiri SH, Amiri M. A new method for multiobjective optimization based on learning automata. World Acad Sci, Eng Technol 2009.
[37] Wu QH, Liao HL. Function optimisation by learning automata. Inform Sci 2013;220:379–98.
[38] Liao HL, Wu QH. Multi-objective optimization by reinforcement learning. In: Proc of WCCI 2010 IEEE world congr on comput intel, Barcelona, Spain; 2010. p. 3374–81.
[39] Miettinen K. Nonlinear multiobjective optimization. Kluwer Academic Publishers; 1999.
[40] Zitzler E, Thiele L. Multiobjective evolutionary algorithms: a comparative case study and the strength pareto approach. IEEE Trans Evol Comput 1999;3(4):257–71.
[41] Durillo JJ, Nebro AJ, Coello CAC, Garcia-Nieto J, Luna F, Alba E. A study of multi-objective metaheuristics when solving parameter scalable problems. IEEE Trans Evol Comput 2010;14(4):618–35.
[42] Yang S, Li C. A clustering particle swarm optimizer for locating and tracking multiple optima in dynamic environments. IEEE Trans Evol Comput 2010;14:959–74.
[43] Shi L, Wang C, Yao L, Wang L, Ni YX, Masoud B. Optimal power flow with consideration of wind generation cost. In: Proc of the 2010 int conf on power syst technol; 2010. p. 1–5.